CRYSTAL GROWTH & DESIGN

pubs.acs.org/crystal

Article

Halogen-Bonded Thiophene Derivatives Prepared by Solution and/or Mechanochemical Synthesis. Evidence of N···S Chalcogen Bonds in Homo- and Cocrystals

Shiv Kumar, Carole Body, Tom Leyssens, Kristof Van Hecke, Gilles Berger, Arie Van der Lee, Danielle Laurencin, Sébastien Richeter, Sébastien Clément, and Franck Meyer*

Cite This: https://doi.org/10.1021/acs.cgd.2c01402

Read Online

ACCESS | Metrics & More | Article Recommendations | Supporting Information

ABSTRACT: Thiophene, a key building block for the construction of conjugated materials, has been scarcely studied in halogen bonding (XB)-driven self-assemblies. In the present study, two thiophene derivatives modified at position 3 were (co-)crystallized using complementary XB donor/acceptor functional groups. Single-crystal X-ray diffraction analysis confirmed the presence of halogen and chalcogen bonding acting, in most cases, concomitantly. While the majority of the structures are governed by the conventional N···I motif, additional S···N and S···S contacts encouraged the cohesion of the supramolecular architectures. Density functional theory calculations shed the light on interaction energy, their respective contributions of the motifs to these non-covalent bonds, and the overall stability of these assemblies. To gain further insight into the formation and evidence of XB interactions, solution and mechanochemical syntheses of polymorphic adducts were performed, followed by ^{13}C solid-state NMR analysis. Further, ^{1}H and $^{19}F\{^{1}H\}$ solution-state NMR spectroscopy studies were carried out to highlight these interactions in the solution phase. The strength and directionality of halogen bonding thus reaffirm its role as a structure-directing agent for designing functional materials. The evidence of N···S chalcogen bonds in thiophene derivatives also broadens up the horizon of supramolecular chemistry in S-heterocycles, while necessitating further investigation for rational application in materials science.

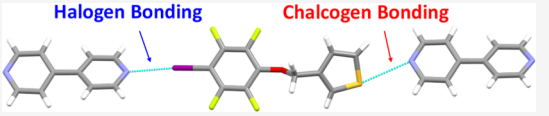

INTRODUCTION

The fabrication of next-generation nanoelectronic devices requires precise control over the reorganization of its active layer components at the nanometer scale.[1] To achieve this goal, "top-down" or "bottom-up" approaches represent the two main strategies to create highly ordered two- or three-dimensional nanostructures.[2] The former strategy is deemed to be too costly to reach a degree of miniaturization lower than 10 nm by a lithographic approach,[3] whereas the latter approach can be highly cost effective and reliable owing to the self-assembly of purposely built elemental constituents through recognition processes.[4,5] The "bottom-up" approach for the construction of nanoscale architectures can thus benefit from the wide array of non-covalent interactions available in the supramolecular chemistry toolbox.[6]

Now, it is well established that the electron donating or accepting strength of a substituent affects the energetics of a π-conjugated semiconducting material.[7] Among the various molecular design principles to tune the band gap and improve the charge transport in organic semiconducting materials, the fluorine substitution stands out as a very appealing strategy by both lowering the highest occupied molecular orbital and the lowest unoccupied molecular orbital level and also acting on morphological aspects by intra- or intermolecular S···F, H···F, F···F, or π···F interactions.[8] Simultaneously, halogen bonding (XB), that is, the ability of a halogen to act as an electron density acceptor, has accounted for an upsurge of interest in the scientific community in the last 2 decades.[9,10] This interaction was initially reported as an intermolecular force in crystal engineering. In subsequent studies, some remarkable features of XB like high directionality, hydrophobicity, or tunable strength were observed and harnessed successfully in biological and materials sciences.[11,12] In the field of organic electronic materials, XB has already been used to guide the arrangement of molecules, as observed in tetrathiafulvalene chemistry.[13] In the same spirit, an improved 3D organization of poly(3-(ω-bromoalkyl)thiophenes) compared to poly(3-alkylthiophenes) has been attributed to S···Br contacts.[14] From a physical point of view, XB was found to enhance the performance of perovskite and dye-sensitized solar cells through reduction of the recombination rate constant and regeneration of the dye, respectively, due to X···I^- interactions (X = Cl, Br, I).[15,16] Halogenation can thereby exert different levels of control over the performance of these functional materials.

Received: November 30, 2022
Revised: January 23, 2023

Thiophene derivatives are versatile and key constituents of many organic semiconducting materials.[17,18] It has already been demonstrated that the supramolecular features of these building blocks can be translated at the macromolecular level to govern the organization of corresponding unit-containing polymers.[19,20] With this in mind, we decided to investigate the supramolecular organization of modified thiophene with the groups prone to interact by halogen bonding.[21] Several studies have already reported the X-ray structures of halogen-bonded arrays based on brominated thiophenes at positions 2 and/or 5, along with other bromine-containing analogues.[22] Herein, we turned our attention toward the thiophene functionalized at position 3 with pyridyl (4-(thiophen-3-ylmethoxy)pyridine, **ThioPy**) and tetrafluoroiodobenzene (3-((2,3,5,6-tetrafluoro-4-iodophenoxy)methyl)thiophene, **ThioI**) groups in combination with complementary XB donor or acceptor partners.[23] We performed the synthesis of polymorphic adducts by solution and mechanochemical approaches and analyzed them by single-crystal and powder X-ray diffraction (PXRD) as well as ^{13}C solid-state NMR (SSNMR). Interestingly, in some of the complexes, both the halogen and chalcogen bonds (ChBs) were teamed up to form supramolecular self-assembly. The occurrence of halogen bonding interactions in the solution phase was also investigated by NMR spectroscopy. Density functional theory (DFT) investigations were employed to emphasize their respective contributions to the formation of these supramolecular architectures.[24,25] Local energy decomposition (LED) analysis (DFT/DLPNO-CCSD(T)/def2-TZVP/Def2-TZVP/C) was performed on fully optimized self-assembled crystal structures to quantify the interactions. Details of specific intermolecular interactions and stabilization energies (Gibb's free energy) of these supramolecular self-assemblies are presented.

EXPERIMENTAL SECTION

Materials. 3-Thiophenemethanol (98%, CAS registry no. 71637-34-8) was obtained from Merck, Belgium. 4-Chloropyridine hydrochloride (97%, CAS registry no. 7379-35-3) was obtained from BLD Pharma, Belgium. Iodopentafluorobenzene (99%, CAS registry no. 827-15-6) was obtained from Fluorochem, UK. Sodium hydride (60%, dispersion in Paraffin Liquid, CAS registry no. 7646-69-7) and potassium *tert*-butoxide (>97%, CAS registry no. 865-47-4) were obtained from TCI Chemicals, Belgium. Tetrahydrofuran (99.5%, extra dry over molecular sieve, stabilized, AcroSeal, ACROS Organics, CAS registry no. 109-99-9, 128-37-0) was obtained from Fisher Scientific. Dimethyl sulfoxide (99.9+%, CAS registry no. 67-68-5) was obtained from Chem-Lab Analytical NV, Belgium. All materials were used as received. Air-sensitive reactions were performed using standard Schlenk techniques under an argon atmosphere. Flash column chromatography was carried out using silica gel (60 Å, 70−200 μm) purchased from DAVISIL—Grace GmbH, Germany. Analytical thin-layer-chromatography was performed using silica plates with aluminum backings (250 μm with F-254 indicator) and were visualized using a 254/365 nm UV lamp.

Solution NMR spectroscopy analyses were performed at the Laboratoire de Mesures Physiques of the University of Montpellier in France and at the Centre d'Instrumentation en REsonance Magnétique (CIREM) of the Université Libre de Bruxelles in Belgium. ^{1}H, $^{13}C\{^{1}H\}$, and $^{19}F\{^{1}H\}$ NMR spectra were recorded on Bruker 300 MHz Avance III HD, 500 MHz AVANCE III or 600 MHz AVANCE III, and JEOL 400 Hz spectrometers at 298 K. $CDCl_3$ was used as received (purchased from Eurisotop, France). ^{1}H and $^{13}C\{^{1}H\}$ NMR spectra were calibrated to TMS on the basis of the relative chemical shift of the residual non-deuterated solvent, used as an internal standard. Chemical shifts (δ) are expressed in ppm from the residual non-deuterated solvent signal, and coupling constants values (^{n}J) are expressed in Hz. Abbreviations used for NMR spectra are as follows: s, singlet; m, multiplet.

The SSNMR spectra were recorded at the Institut Charles Gerhardt in France on a VNMRS 600 MHz (14.1 T) NMR spectrometer using a Varian 3.2 mm probe tuned to ^{1}H (599.82 MHz) and ^{13}C (150.81 MHz) and working under magic angle spinning (MAS) at a spinning rate of 18 kHz. The temperature control unit was set to ∼0 °C during all measurements. The cross-polarization (CP) MAS sequence was used, with a contact time (CT) of 0.2 or 4 ms, allowing to distinguish ^{13}C resonances depending on their relative proximity to protons in the crystal structure (and thereby identifying the $^{13}C-I$ resonance in particular). Recycle delays used were adapted sample by sample (with values as long as 400 s for **ThioPy**). The number of transients acquired ranged from 126 to 826, depending on the sample and CT. ^{13}C chemical shifts were referenced to adamantane, used as a secondary reference (high-frequency peak at 38.5 ppm with respect to tetramethylsilane).

Melting points were measured using one side open-ended capillaries on a Buchi melting point B-545 apparatus and are uncorrected.

Ball Milling in Neat Grinding and LAG Conditions. Grinding was performed on a Retsch MM400 using a grinding frequency of 30 Hz for a period of 90 min. About 19.12 mg of **ThioPy** (0.1 mmol, 1 equiv) and 38.81 mg of **ThioI** (0.1 mmol, 1 equiv) were placed in a polypropylene Eppendorf of 2 mL, to which 3 grinding stainless-steel beads of 3 mm were added. 10 μL of solvent was added to all except the neat sample.

Differential Scanning Calorimetry. Differential scanning calorimetry (DSC) measurements were performed on a TA DSC2500 instrument. Samples were deposited in the aluminum Tzero pans with a punctured lid and heated from 25 up to 100 °C using a heating rate of 20 °C/min under a 50 mL/min continuous nitrogen flow.

Single-crystal XRD Analysis. The crystal evaluation and data collection of **ThioI** (at 175 K) and **ThioPya** (at 173 K) were performed on a Rigaku Oxford-Diffraction Gemini-S diffractometer with sealed-tube Mo Kα (λ = 0.71073 Å) radiation using the CrysAlis Pro program (Rigaku Oxford-Diffraction, 2012).[26] This program was also used for the integration of the data using default parameters for the empirical absorption correction using spherical harmonics employing symmetry-equivalent and redundant data and the correction for Lorentz and polarization effects. The ab initio iterative charge flipping method was used to solve the crystal structures with parameters described elsewhere[27] employing the Superflip[28] program, and they were refined using full-matrix least-squares procedures on structure factor amplitudes F as implemented in CRYSTALS[29] using all independent reflections with $I > 2\sigma(I)$. The thiophene rings appeared to be positionally disordered with respect to the sulfur atoms and the neighboring carbon atom. The site occupancy factors S/C were 0.717(4)/0.283(4) and 0.671(2)/0.329(2) for **ThioI** and **ThioPya**, respectively.

For the structures of **ThioPy−1,2TFIB**, **ThioPy−1,4TFIB**, **ThioPy−diIC4**, **ThioPy−diIC6**, **ThioI−BiPy**, **ThioI−BiPyethy**, **ThioI−BiPyetha**, and **ThioPyb**, X-ray intensity data were collected at 100 K on a Rigaku Oxford Diffraction Supernova Dual Source (Cu at zero) diffractometer equipped with an Atlas CCD detector using ω scans and Mo K_α (λ = 0.71073 Å) radiation. The images were interpreted and integrated with the program CrysAlisPro.[30] Using Olex2,[31] the structures were solved by direct methods using the ShelXT structure solution program and refined by full-matrix least squares on F^2 using the ShelXL program package.[32,33] Non-hydrogen atoms were anisotropically refined, and the hydrogen atoms were in the riding mode with isotropic temperature factors fixed at 1.2 times U(eq) of the parent atoms.

Mechanochemical Synthesis and X-ray Powder Diffraction Analyses of ThioI−ThioPy Complexes. The X-ray powder diffraction analyses were carried out with a Siemens D5000 diffractometer equipped with a Cu cathode (λ(Cu Kα) = 1.5418 Å), operating at 40 kV and 40 mA and using a Bragg Brentano geometry.

https://doi.org/10.1021/acs.cgd.2c01402
Cryst. Growth Des. XXXX, XXX, XXX−XXX

Scheme 1. Syntheses of Thiophene Derivatives ThioPy and ThioI (Top)[a]

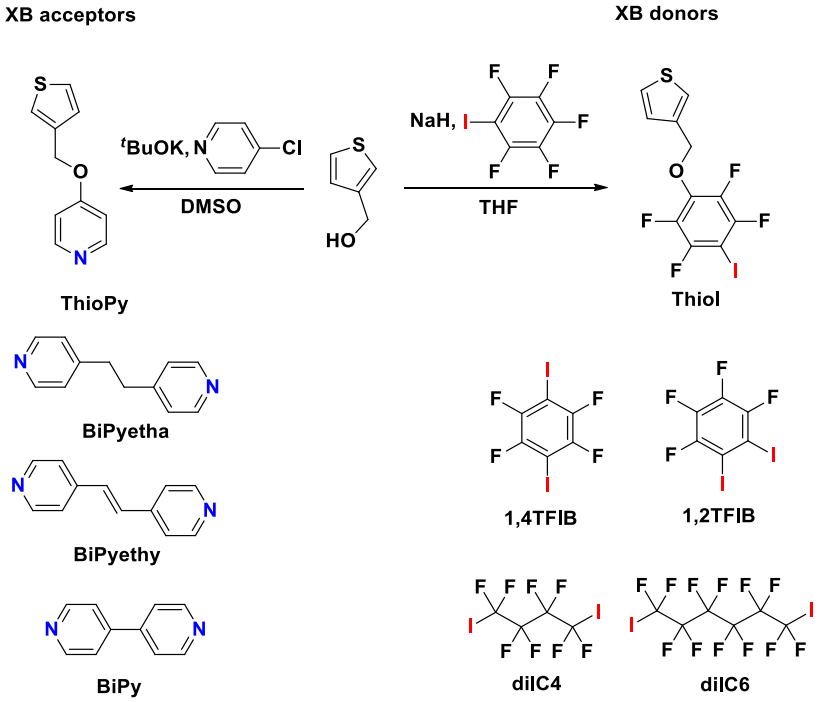

[a]Halogen bond donors (red) and acceptors (blue) were used in this study (bottom).

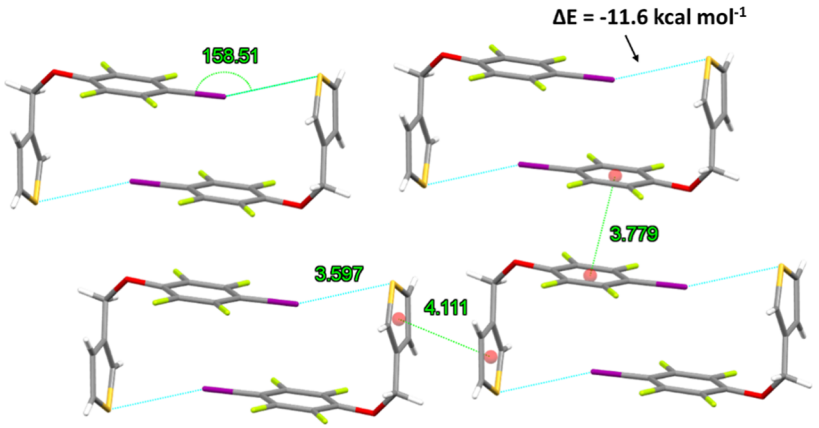

Figure 1. Packing arrangement in the X-ray structure of **ThioI** at 175 K developing circular motifs due to S···I halogen bonds. The red dots represent the centroid of the aromatic rings. Colors are as follows: C, gray; H, white; F, yellow; S, orange; O, red; I, purple. Minor components of disordered thiophene rings in **ThioI** have been omitted for clarity.

The small shifts in the positions of the diffraction peaks in the products recovered after ball-milling, compared to the simulations done from the single-crystal XRD data, can be due to the difference in analysis conditions (especially temperature).

Cambridge Structural Database Survey (Version 2021.1, 5.42 Updates May 2021). A single query was built using ConQuest via the Draw option and searching for N···S distances lower than 3.35 Å for compounds possessing thiophene and pyridyl rings. This was done by defining an intermolecular contact (up to exactly 3.35 Å) between the thiophene S-atom and pyridyl N-atom. The search (using no additional filters) returned the following hitlist with refcodes:

FAJDED, AJUMAT, APUSUB, DELDEG, DUBTIF, FOPZUI, LODREE, NOTFOT, QOWNOI, QUDSOX, RAVTAJ, TASTIR, WITVAY, XIGVIV, and YODFAB. NOTFOT and XIGVIV involve pyridinium derivatives.

Theoretical Methods. All calculations were carried out using ORCA 5.0.2 package as single points from the X-ray geometries.[34,35] LED analysis was then performed to assess interaction energies at the domain-based local pair natural orbital level of theory [DLPNO-CCSD(T)][36,37] using the tight PNO setting, the def2-TZVP basis set,[38] and the corresponding auxiliary bases for the resolution of identity approximation, exchange, and Coulomb fitting.

The interaction energies have been calculated as previously reported.[37] EintraX and EintraY are the electronic energies of both fragments in the complex, E_x and E_y are the energies of the isolated fragments, and E_{prep} is the required energy from the isolated ground state to the electronic structure in the interacting fragments. ΔE_{xy} is the final interaction energy.

RESULTS AND DISCUSSION

The synthesis of 3-((2,3,5,6-tetrafluoro-4-iodophenoxy)-methyl)thiophene (**ThioI**) and 4-(thiophen-3-ylmethoxy)-pyridine (**ThioPy**) as XB donor and acceptor, respectively, was carried out according to a procedure already described in the literature (Scheme 1).[21]

https://doi.org/10.1021/acs.cgd.2c01402
Cryst. Growth Des. XXXX, XXX, XXX−XXX

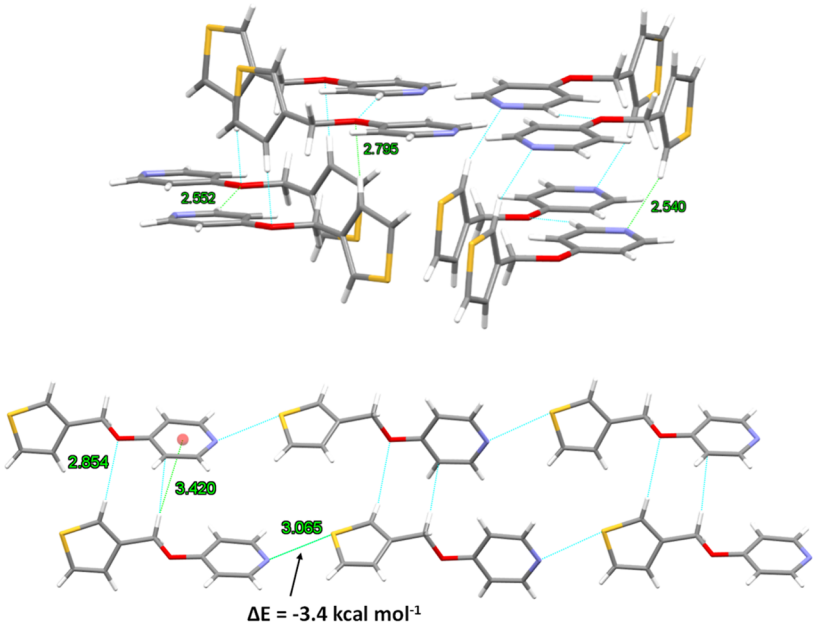

Figure 2. Packing arrangement in the X-ray structures of the two **ThioPy** polymorphs developing a herringbone pattern due to H···O hydrogen bonds in **ThioPya** (top, at 173 K) and a linear arrangement due to S···N chalcogen bonds in **ThioPyb** (bottom, at 100 K). Colors are as follows: C, gray; H, white; N, blue; S, orange; O, red. Minor components of disordered thiophene rings in both structures have been omitted for clarity.

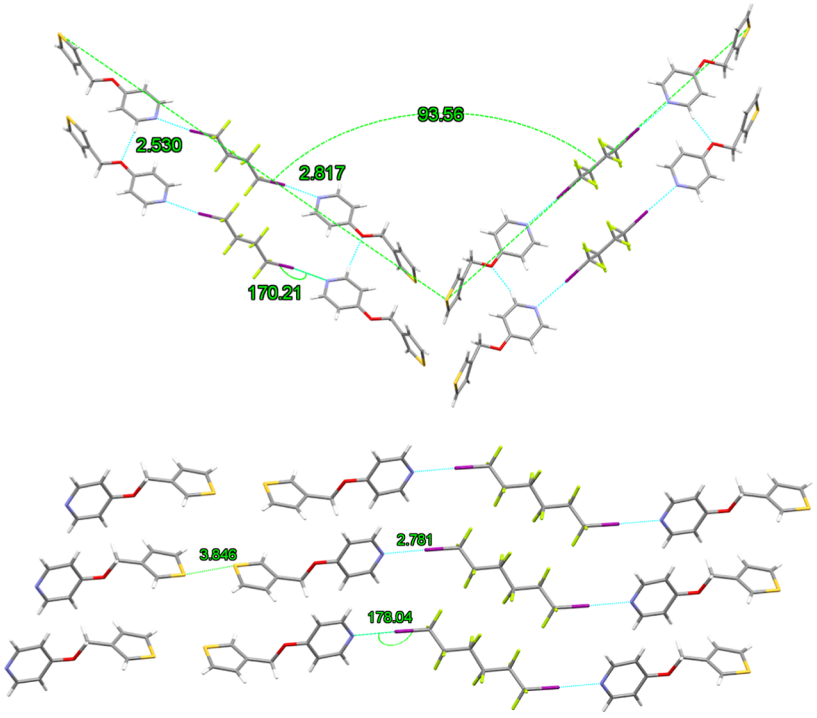

Figure 3. Packing arrangement in the X-ray structures of halogen-bonded complexes **ThioPy−diIC4** (top, at 100 K) and **ThioPy−diIC6** (bottom, at 100 K). Minor components of disordered thiophene rings in both structures and **diIC4** have been omitted for clarity.

Single-Crystal XRD Analysis of ThioI. Subsequently, the high-quality single crystals suitable for XRD analysis of halogenated thiophene derivative, **ThioI**, were obtained through slow evaporation of dichloromethane solution. **ThioI** units follow a S···I XB-driven supramolecular structure (Figure 1). The S···I distance (3.597 Å) is around 5% shorter than the sum of van der Waals radii, and the S···I−C angle is about 158°, which is consistent with the electron donation from sulfur to iodine (interaction energy ∼−11.6 kcal mol^{-1}, Table S5).[39]

The S···I contact seems to govern the supramolecular arrangement of paired molecules into circular motifs. Each unit adopts an L-shape conformation in which the thiophene and tetrafluoroiodobenzene groups are almost perpendicular (∼78°) (Figure S1). The overall architecture is also supported by π-stacked thiophenes (centroid distance = 4.111 Å) and

https://doi.org/10.1021/acs.cgd.2c01402
Cryst. Growth Des. XXXX, XXX, XXX−XXX

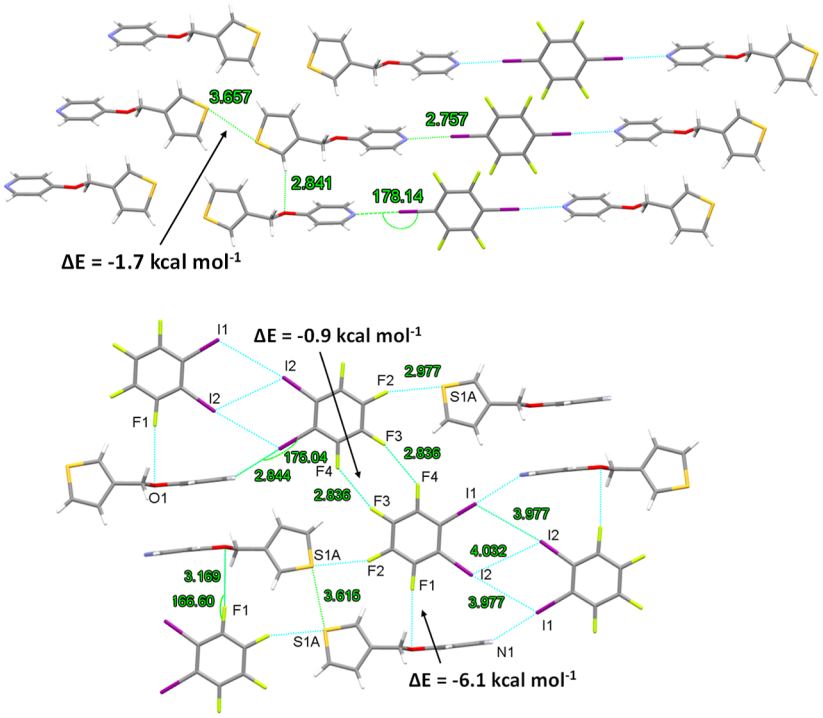

Figure 4. Packing arrangement in the X-ray structures of halogen-bonded complexes **ThioPy−1,4TFIB** (top, 100 K) and **ThioPy−1,2TFIB** (bottom, at 100 K). Minor components of disordered thiophene rings in both structures have been omitted for clarity.

perfluoroarenes (centroid distance = 3.779 Å) belonging to neighboring pairs.

After determining the effective role of **ThioI** as a halogen bond donor, the single-crystal structure of **ThioPy** was then studied. Interestingly, two crystallization attempts of **ThioPy** in dichloromethane and a dichloromethane/*n*-hexane mixture gave rise to polymorphic forms called **ThioPya** and **ThioPyb**, respectively. In the first case, thiophene units of **ThioPya** develop a planar arrangement in a herringbone style due to H···O hydrogen bonds (2.552 Å) linking adjacent molecules (Figure 2 top).

This supramolecular architecture is further stabilized by additional H···N and H···O hydrogen bonds with distances of 2.540 and 2.795 Å, respectively, involving molecules of parallel planes. On the other hand, the X-ray analysis of the **ThioPyb** single crystal obtained from the solvent mixture revealed a different pattern (Figure 2 bottom). A linear arrangement is obtained due to intermolecular S···N chalcogen bonds. The refined crystal structure highlights a separation of 3.065 Å, which represents 91.5% of the sum of van der Waals radii. According to DFT calculations, the chalcogen bond energy is −3.4 kcal mol^{-1}, which is in the same order of magnitude that was calculated for a thiophene−pyridine complex.[40] Other weak hydrogen bonds, namely, H···O (2.854 Å) and H···π interactions (H···centroid distance = 3.420 Å), operate between the parallel chains. The single-crystal XRD analysis of pure thiophenes **ThioI** and **ThioPy** confirmed the role of the aromatic groups as structure-directing agents for these supramolecular assemblies. Next, we investigated the cocrystallization of these building blocks with selected partners.

XRD Analysis of Cocrystals Involving ThioPy and Diiodoperfluorinated Compounds. Halogenoperfluorinated chains are commonly used in halogen bonding-driven self-assemblies. In fact, the strong electron-withdrawing fluorine atoms behave as activating agents toward the associated halogens by increasing their σ-hole size. Furthermore, the rod-like character of the perfluorinated core allows a reliable transfer of molecular information.[41]

First, **ThioPy** and diiodoperfluorobutane (**diIC4**) were cocrystallized, leading to a supramolecular trimeric structure held together by N···I halogen bonds (Figure 3 top). The distance between these two atoms is 2.817 Å, which is about 20% shorter than the sum of van der Waals radii, and the N···I−C angle is almost linear (∼170°). In this particular complex, we can consider that S and N compete to make XB with I, but the strongest prevails. These trimeric systems develop undulating chains making an angle of about 93° with thiophene rings at both extremities pointing toward one another, as observed in **ThioPya**. The stabilization of this architecture is further ensured by weak H···O hydrogen bonds (2.530 Å) that link parallel trimers. Subsequently, we studied the self-assembly of **ThioPy** with a longer analogue, that is diiodoperfluorohexane (**diIC6**) (Figure 3 bottom). In a similar way, the telechelic perfluorinated unit links both compounds into a trimeric structure due to N···I halogen bonds. The N···I separation drops to 78% of the sum of van der Waals radii, and the N···I−C angle makes ∼178°. However, a comparison of **ThioPy−diIC4** and **ThioPy−diIC6** at the macromolecular level highlights a different organization.

The repetition of the trimeric architecture forms infinite parallel chains with two thiophene rings pointing toward each other. The S···S separation is measured at 3.846 Å, which is slightly longer than the sum of van der Waals radii. In **ThioPy−diIC6**, all units belonging to parallel planes run in the same direction, which contrasts with **ThioPy−diIC4** and its zig-zag motif (Figure S2). The planar organization features a clear segregation between **ThioPy** and **diIC6**, emphasizing the low affinity between perfluorocarbons and hydrocarbons. It is worth noting that this aspect is consistent and observed in **ThioPy−diIC4** as well.

https://doi.org/10.1021/acs.cgd.2c01402
Cryst. Growth Des. XXXX, XXX, XXX−XXX

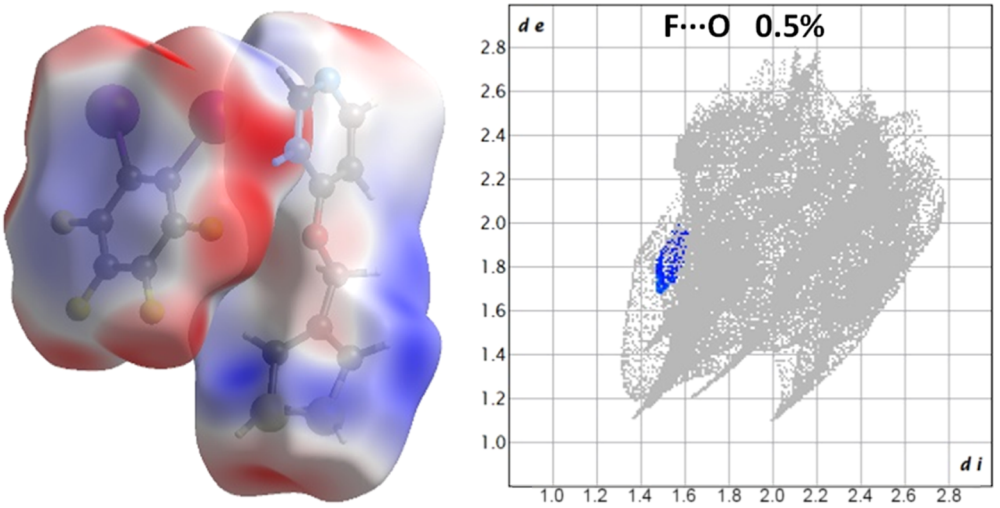

Figure 5. Hirshfeld surface of the **ThioPy−1,2TFIB** complex displaying an overlapping electron density of a F atom of **1,2TFIB** with an O atom of **ThioPy** (left). Two-dimensional fingerprint plot for F···O interactions (right).

We then turned our attention toward diiodoperfluoroarenes. In particular, 1,4-diiodotetrafluorobenzene (**1,4TFIB**) belongs to a class of halogen bond donors that have been frequently engaged in supramolecular functional materials.[42] Some relevant findings concern its role in the construction of organic cocrystal micro-lasers and haptic memory materials.[43,44] Interestingly, **ThioPy−1,4TFIB** complexes develop a similar linear organization as **ThioPy−diIC6** (Figure 4 top); halogen bonding parameters appear almost identical (N···I distance = 2.757 Å, N···I−C angle ∼178°), while the distance that separates the thiophene groups turns out to be shorter. Now, the S···S contact is measured at 3.657 Å, which is within the limit of the sum of van der Waals radii (interaction energy ∼−1.7 kcal mol^{-1}, Table S5).

Although all three diiodoperfluorinated compounds (**diIC4**, **diIC6**, and **1,4-TFIB**) used in the formation of self-assemblies are linear in geometry, it remains difficult to explain the structural variation from zig-zag (**ThioPy−diIC4**) to linear (**ThioPy−1,4TFIB** and **ThioPy−diIC6**) chains with these results. The absence of conjugation in the **ThioPy** core prevents any competitive/cooperative phenomenon of electron transfer from intermolecular interactions.[45] Further investigations are under progress to explain this structural variation. The use of 1,2-diiodotetrafluorobenzene (**1,2TFIB**) as an XB building block has been reported less frequently than **1,4TFIB**, probably due to the difficulty to anticipate the geometry of the resulting complex. However, recent works have highlighted its potential in inducing phosphorescence in the presence of diazaphenanthrenes and the self-organization of photoresponsive block copolymers.[46,47] The cocrystal formation involving **ThioPy** and **1,2TFIB** led to a supramolecular architecture with a complex packing pattern. In this case, a multitude of noncovalent bonds coexist, in which almost all halogen atoms of **1,2TFIB** are involved. As expected, **ThioPy** and **1,2TFIB** were linked through strong N···I interactions, but only one iodine atom is involved, which is rather uncommon in light of the literature (Figure 4 bottom).[48] The refined crystal structure parameters show a N···I separation of 2.844 Å (∼80% of the sum of van der Waals radii) and an N···I−C angle of 175°. In addition, the short distances between iodine atoms arise within the limit of precision for halogen bonds of types I and II, taking into consideration the sum of van der Waals radii for iodine (3.96 Å). Since the distance between I1 and I2 is 3.977 Å and the C−I1···I2 and C−I2···I1 angles are 119.2 and 173.9°, respectively, the halogen−halogen interactions between I1 and I2 can be concluded, by definition, as XB type II contacts. A weak halogen−halogen interaction present between two I2 atoms exhibits XB type I as revealed by a distance of 4.032 Å and identical C−I2···I2 angles of 118.9°.[49] Surprisingly, F1 points toward the oxygen atom of **ThioPy**, but the distance (3.169 Å) appears slightly longer than the sum of van der Waals radii (O + F = 2.99 Å).[50,51] It is worth mentioning that examples showing a fluorine atom as a halogen bond donor are scarce in the literature.[52,53] For instance, the first examples of $C_{sp3}F\cdots O_{sp3}$ interactions were reported in palladium complexes only in 2019.[54] Despite the longer distance than the sum of van der Waals radii between O and F, using the Hirshfeld surface representation, we were able to successfully establish that there is indeed an F···O interaction in the **ThioPy−1,2TFIB** complex (Figure 5).[55] We were also able to quantify the contribution of overlapped surface area to 0.5% in total electrostatic potential surface, and the calculated interaction energy was determined to be around −6.1 kcal mol^{-1}. Finally, S···S and S···F2 chalcogen bonds of 3.638 and 2.988 Å, respectively, lock the structure and give rise to a planar organization of these modules.

XRD Analysis of Cocrystals Involving ThioI and Bipyridyl Derivatives. Next, we decided to investigate the self-assemblies by reversing the XB counterparts through **ThioI** and bipyridyl derivatives, namely, bipyridine ethane (**BiPyetha**), bipyridine ethylene (**BiPyethy**), and bipyridine (**BiPy**). The self-assembly of **ThioI** with **BiPyetha** was allowed to form in a dichloromethane/*n*-hexane mixture using a 2:1 ratio. As expected, the refinement of single-crystal XRD data analysis revealed a similar arrangement as the one found for **ThioPy−diIC6** (Figure 6 top). This trimeric system (**ThioI···BiPyetha···ThioI**) forms an almost linear geometry with a N···I−C angle of ∼174° and an interatomic distance of 2.791 Å (79% of the sum of van der Waals radii) due to N···I halogen bond (interaction energy ∼−6.7 kcal mol^{-1}, Table S5). In the same way, the successive trimer modules develop a chain with thiophene rings pointing toward each other. The S···S separation is slightly shorter than in **ThioPy−diIC6** (3.728 Å), but it remains longer than the sum of van der Waals radii

https://doi.org/10.1021/acs.cgd.2c01402
Cryst. Growth Des. XXXX, XXX, XXX−XXX

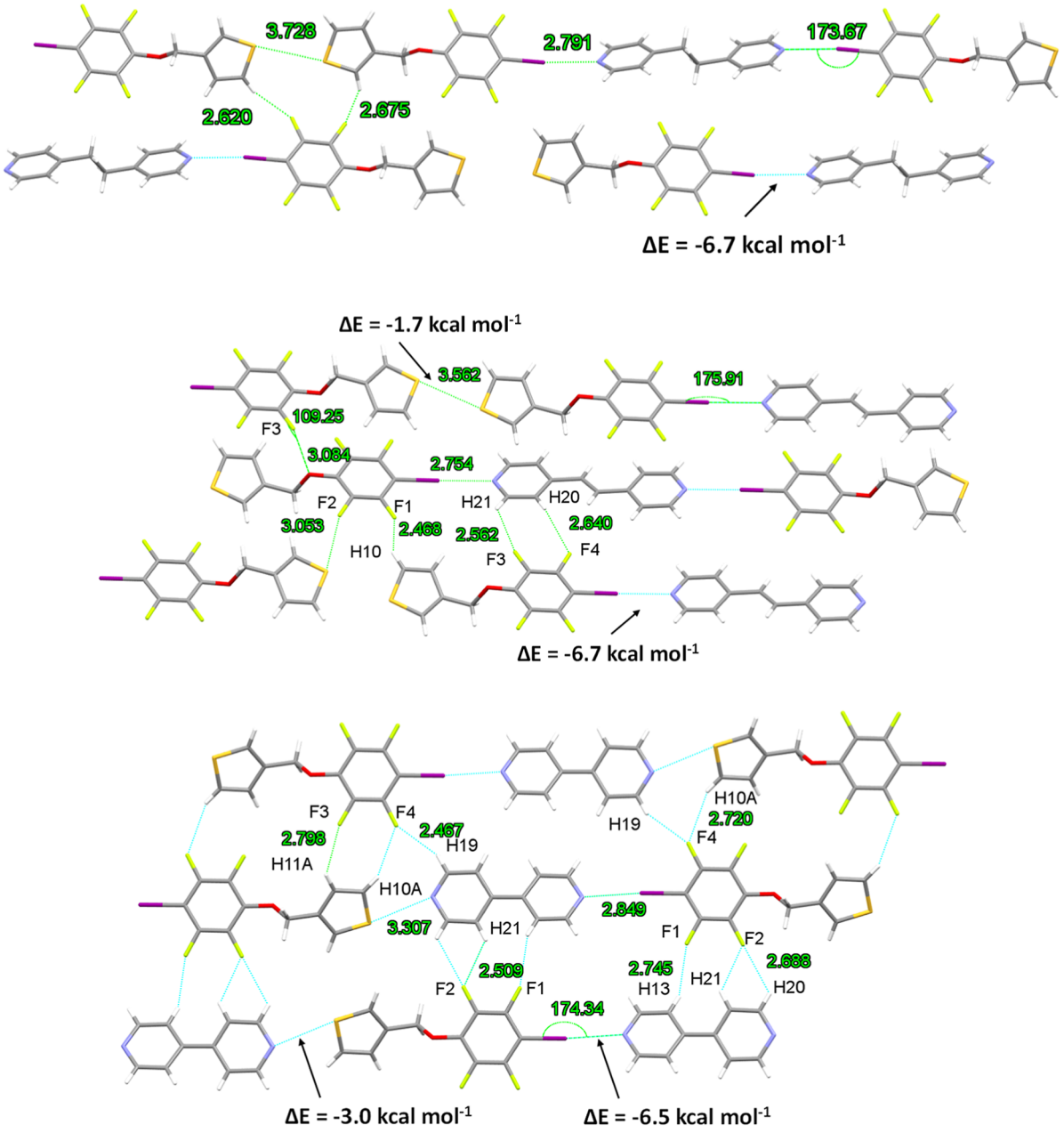

Figure 6. Packing arrangement in the X-ray structures of halogen-bonded complex **ThioI−BiPyetha** (top, at 100 K), **ThioI−BiPyethy** (middle, at 100 K), and **ThioI−BiPy** (bottom, at 100 K). Minor components of disordered thiophene rings in **ThioI−BiPyetha** and **ThioI−BiPy** have been omitted for clarity.

for S. These thiophene groups are also hydrogen-bonded with a neighboring **ThioI** unit due to two H···F contacts of 2.620 and 2.675 Å, respectively.

Following the same protocol, **ThioI** and **BiPyethy** were cocrystallized under the same conditions. The supramolecular organization was mirrored as observed for **ThioI−BiPyetha** (Figure 6 middle).

The N···I interactions held the three units together, and the refined single-crystal XRD data analysis corroborated with a halogen bonding between N and I (N···I distance = 2.754 Å and N···I−C angle ∼176°) (interaction energy ∼−6.7 kcal mol^{-1}, Table S5). Likewise, the linear arrangement reveals thiophene rings pointing toward each other, but in contrast to the previous case, the S···S distance is now lower than the sum of van der Waals radii (3.562 Å). The attractive nature of this contact is attested by a weak interaction energy of about −1.7 kcal mol^{-1} (Table S5). This architecture is also composed of other weak contacts linking parallel chains to one another. The S···F2 chalcogen bonds with an average bond length of 3.053 Å (∼7% interactions of the sum of van der Waals radii) are supplemented by three H···F hydrogen bonds with bond lengths of 2.468 Å (H10···F1), 2.562 Å (H21···F3), and 2.640 Å (H20···F4), respectively. As for **ThioPy−1,2TFIB**, two thiophenes belonging to parallel planes show a short O···F distance of only 3.084 Å (O···F4−C angle ∼109°).

Last, **ThioI−BiPy** highlighted the most surprising system (Figure 6 bottom). In comparison to the other **ThioI−**bipyridine adducts studied here, this particular module develops a linear arrangement not just with N···I interactions even supplemented by N···S chalcogen bonds, leading to

https://doi.org/10.1021/acs.cgd.2c01402
Cryst. Growth Des. XXXX, XXX, XXX−XXX

infinite chains running in opposite directions. XB is slightly weaker than in the previous complexes (N···I distance = 2.849 Å and N···I−C angle ∼174°), and the calculated interaction energy was found to be approximately −6.5 kcal mol^{-1} (Table S5). The N···S distance (3.307 Å) represents a very weak interaction considering the sum of van der Waals radii (S + N = 3.35 Å). According to DFT calculations, the chalcogen bond energy is around −3.0 kcal mol^{-1}, contributing substantially to the crystal cohesion.[40] In that complex, parallel chains are also stabilized due to a plethora of H···F hydrogen bonds. This unexpected self-assembly convinced us to get more information on such intermolecular N···S contacts through a CSD survey.

N···S Chalcogen Bonds in the CSD. In the last few years, the chalcogen bonds have gained significant attention in chemical sciences and protein−ligand complexes due to their similarities with the halogen bonds, notably due to an anisotropic charge distribution.[56,57] Typically, the ability of an element of group 16 to form chalcogen bonds depends upon the nature of neighboring residues. Hence, electron-withdrawing groups tend to increase the size of the positive σ hole on the chalcogen atom and give rise to stronger attractive interactions. Moreover, the elements like selenium (Se) and tellurium (Te) are more polarizable chalcogen atoms than S, which makes the latter less prone to form a chalcogen bond through recognition processes.[58] Whereas the intramolecular N···S interactions are frequently encountered in stabilizing a planar conformation (e.g., in conducting materials),[59] the same contacts are rarely reported at the intermolecular level. To find out the frequency of occurrence of the unusual N···S chalcogen bond as observed in **ThioI−BiPy**, a preliminary CSD survey (version 2021.1, 5.42 updates May 2021) was carried out focusing on structures composed of S and N atoms and connected to 2 C atoms with a N···S bond distance smaller than 3.35 Å. As a result, a total number of 181 compounds came out with such inter- or intramolecular interactions. This number dropped to 13 structures when thiophene and pyridine derivatives were considered, and all these were homocrystals (see the Supporting Information). Screening further, we then focused on crystalline systems where two different units are linked through intermolecular N···S interactions and this number further dropped to 5. Only five molecular entities featured the same parameters (N···S distance < 3.35 Å), referred to in the database by the following refcodes: OGUTIV,[60] NAQPUT,[61] FAFSEL,[62] SUKPAS,[63] and NUSLOE.[64] This led us to the conclusion that N···S chalcogen bond-driven self-assemblies of complementary partners arise as a rare phenomenon in crystal engineering.

Mechanochemical Syntheses of ThioI−ThioPy Complexes. Mechanochemistry is one of the important synthetic techniques in modern chemistry to prepare (nano)materials.[65] This technique can produce homogeneous nanosized composite materials at an industrial scale and offers the opportunity to study both the stoichiometric and non-stoichiometric compositions of nanomaterials. As mentioned in the introduction, controlling and understanding the formation of different polymorphs are crucial aspects considering the associated structure−property relationship at the molecular or bulk level. The supramolecular organizations of two polymorphic structures of complementary thiophenes **ThioI−ThioPy** (called **ThioI−ThioPy A** and **ThioI−ThioPy B**, see Figures S3 and S4) have already been studied in previous work.[21] Single crystals of **ThioI−ThioPy A** and **ThioI−ThioPy B** were grown from dichloromethane/*n*-hexane and acetone, respectively. However, the scaling up of the solution-based synthesis of such complexes is a challenge. Therefore, complex **ThioI−ThioPy** was considered as a model system to investigate how the mechanochemistry conditions can exert a control on polymorphic outcome. To purposely address these issues, the mechanochemical synthesis of **ThioI−ThioPy** was carried out by ball milling in neat conditions and also through a liquid-assisted grinding approach (LAG) method using methanol, toluene, THF, water, and dichloromethane (ca. 0.2 μL/mg). Subsequently, the produced materials were characterized by PXRD and compared with the starting compounds as well as **ThioI−ThioPy** complexes obtained by solution synthesis (see Figures S5−S14).

As a result, **ThioI−ThioPy A** was obtained under a neat and methanol-assisted grinding process, whereas **ThioI−ThioPy B** formed only by the LAG method in the presence of toluene, THF, water, and dichloromethane as a solvent (Table 1). In a mechanochemical synthesis performed under LAG conditions, the protic/aprotic character and polarity of the added solvent can influence the yielded forms. But, in our case study, no clear trend could be observed considering the results that show that highly polar and protic methanol and water led to two different polymorphs. Both polymorphs were found to be stable at room temperature in the solid state for over a month (Figure S13). On the other hand, when creating a supersaturated suspension in acetone containing both forms A and B, a complete transformation of form B to form A was observed, showing the latter to be the thermodynamically stable form at this temperature and in this solvent environment (Figure S14). This solvent was chosen as the cocrystal behaves congruently in this solvent. Last, it is worth mentioning that both forms show similar melting temperatures of 69 °C, which lies in between the melting points of **ThioI** (63 °C) and **ThioPy** (84 °C) (Figures S15−S18). As form A also has the highest melting enthalpy, both forms are likely monotropically related.

Table 1. Preparation of ThioI−ThioPy Complexes by Ball Milling in Neat Grinding Conditions and Using LAG (with ca. 0.2 μL/mg)

conditions	dielectric constants[66,67]	isolated complexes
neat		**ThioI−ThioPyA**
methanol	32.6	**ThioI−ThioPyA**
water	78.5	**ThioI−ThioPyB**
toluene	2.41	**ThioI−ThioPyB**
dichloromethane	8.9	**ThioI−ThioPyB**
THF	7.4	**ThioI−ThioPyB**

^{13}C Solid-State NMR Spectroscopy Analysis. SSNMR spectroscopy has become an important analytical tool that complements PXRD analysis, particularly for disordered systems and structures showing internal dynamics.[68] As far as the study of halogen-bonded complexes is concerned, the SSNMR analyses have proven to be highly informative, especially by looking at the local environments of ^{15}N, ^{13}C, ^{31}P, ^{17}O, and/or ^{35}Cl SSNMR, for example.[69] Here, ^{13}C SSNMR analyses were carried out for solid samples of **ThioI**, **ThioPy**, and **ThioI−ThioPy** to highlight the XB. The C−I resonance (C9) is only observed when measurements are performed at longer contact times (CT = 4 ms) due to the absence of a direct bond between the C9 and protons. Moreover, the broadness of this C9 resonance is due to the

https://doi.org/10.1021/acs.cgd.2c01402
Cryst. Growth Des. XXXX, XXX, XXX−XXX

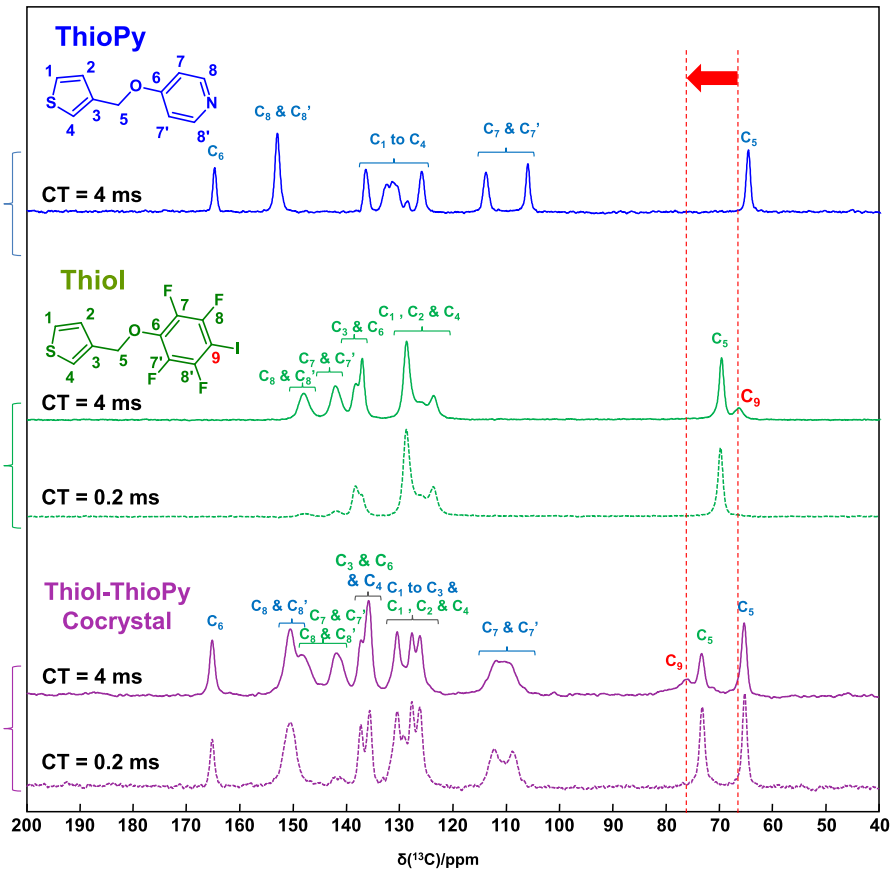

Figure 7. ^{13}C SSNMR spectra of **ThioPy** (blue), **ThioI** (green), and the **ThioI−ThioPy** cocrystal (purple), recorded using CPMAS and different CTs and showing the shift in the C−I resonance (C9) upon the formation of the halogen-bonded cocrystal.

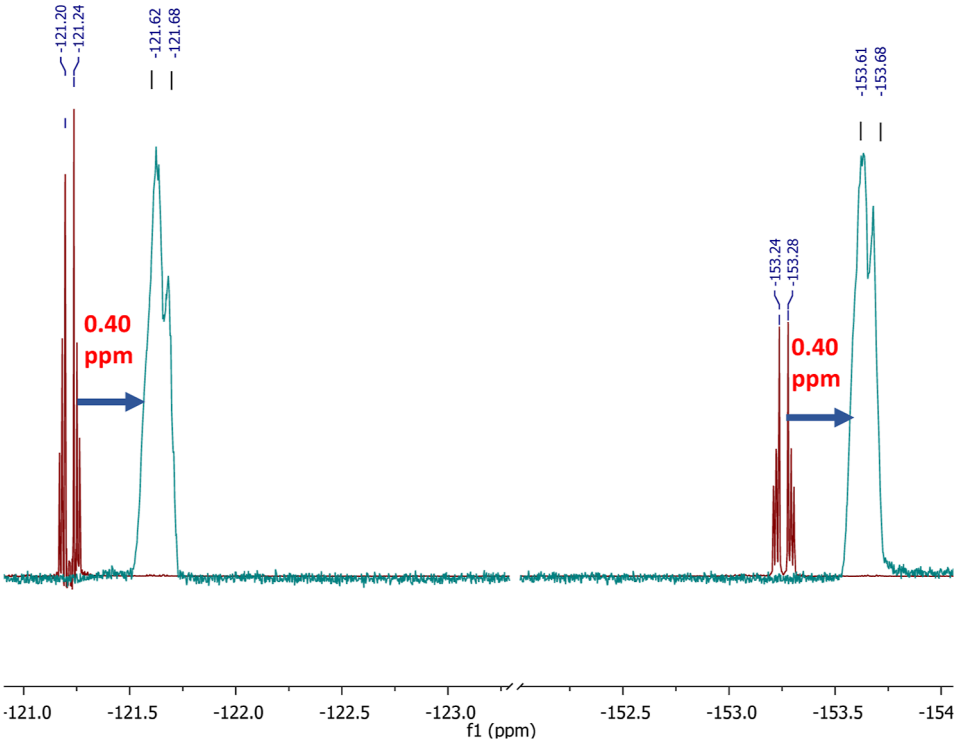

Figure 8. $^{19}F\{^{1}H\}$ NMR spectra of **ThioI**/**TBACl** in $CDCl_3$ suggesting the I···Cl^- halogen bonds (**TBACl** = tetrabutylammonium chloride). Molar ratio (**ThioI**/**TBACl**): 1:0 (red), 1:10 (blue).

https://doi.org/10.1021/acs.cgd.2c01402
Cryst. Growth Des. XXXX, XXX, XXX−XXX

quadrupolar nature of the bound iodine. The ^{13}C SSNMR spectrum of **ThioI**−**ThioPy** exhibits a deshielding of ∼9 ppm of the C9 resonance compared to pure **ThioI**, which is consistent with the formation of a halogen bond, as reported elsewhere (Figure 7).[69,70] A small shielding from 153.1 to 150.7 ppm was also observed for C8 and C8′ of the pyridyl ring, further attesting to the formation of a halogen-bonded cocrystal in the solid state.

XB Interactions in the Solution Phase. After direct evidence of XB in the solid state, efforts were put together to detect these interactions in the solution state. In this regard, the binary systems were studied by UV−visible absorption spectroscopy and solution-state ^{1}H or $^{19}F\{^{1}H\}$ NMR (see the Supporting Information). Because both **ThioI** and **ThioPy** strongly absorb in the same UV region, the UV−visible absorption spectroscopy measurements remained inconclusive to confirm XB interactions in the solution state; therefore, they are omitted. Nevertheless, ^{1}H and $^{19}F\{^{1}H\}$ NMR spectroscopy experiments were successful to confirm the types of interactions acting in the solution state.

ThioI and **ThioPy** were thereby challenged with complementary electron donors, namely, an ammonium chloride and **diIC4**. The shift in $^{19}F\{^{1}H\}$ NMR spectra of **ThioI** and **ThioI**/**TBACl** (ratio 1:10; **TBACl** = *n*-tetrabutylammonium chloride) in $CDCl_3$ suggests the ability of **ThioI** to be engaged in I···Cl^- halogen bonding (Figure 8).[71] This observation broadens up the scope of ion-mediated self-assembly of neutral thiophene-based conductive π-conjugated polymers.

Similarly, the chemical shift in $^{19}F\{^{1}H\}$ NMR spectra of **diIC4** and **diIC4**/**ThioPy** (ratio 1:5) confirms the existence of I···N interaction in the solution phase (Figure S19). In contrast, no chemical shift in $^{19}F\{^{1}H\}$ NMR spectra was observed for the **ThioI**−**ThioPy** XB pair (Figure S20). However, as the relative ratio of **ThioPy** was increased in the **ThioI**−**ThioPy** system, a significant upfield chemical shift for pyridyl hydrogen of the **ThioPy** unit was observed in ^{1}H NMR spectra, indicating strong $\pi-\pi$ interactions in the solution state (Figure S21). The same trend was observed in $^{13}C\{^{1}H\}$ NMR spectra as well (Figure S22). The competition between XB and lone pair (lp)···π interaction in the solution state is well known for aromatic XB donors/acceptors. A downfield trend is expected in solution-state NMR if XB prevails.[72]

CONCLUSIONS

In summary, we have investigated the supramolecular organization of two XB donor/acceptor-modified thiophene derivatives with complimentary XB acceptor/donor components through halogen bonding, prepared via both solution and mechanochemical routes. The XRD analysis of single crystals obtained from the solution confirmed the presence of XB-driven supramolecular self-assemblies. Interestingly, the evidence of chalcogen bonds acting concomitantly with XB and contributing to the crystal cohesion in some adducts was found. Most strikingly, the cocrystal **ThioI**−**BiPy** develops a linear arrangement of alternating units as the result of N···I and N···S noncovalent bonds, with **ThioPyb** being also organized by N···S contacts. A CSD survey further confirmed that the occurrence of such intermolecular N···S contacts is a rare phenomenon and scarcely reported in the literature. Moreover, the theoretical calculations attested to the substantial contribution of this interaction to the supramolecular scaffold. For scaling-up purposes, further insight was sought into the formation and characterization of two polymorphic forms of the **ThioI**−**ThioPy** cocrystal. The mechanochemical synthesis by ball milling in neat grinding conditions and by the LAG method gave rise to both polymorphic forms A and B without any particular relationship with the solvent polarity. The most thermodynamically stable form A was also obtained through a supersaturated suspension in acetone. Mechanochemistry thus offers an appealing alternative to control the organization of the **ThioI**−**ThioPy** complex compared to the solution synthesis. A ^{13}C SSNMR analysis also highlighted the formation of a cocrystal with XB by the variation of C−I (**ThioI**) resonance compared to pure units. Solution-state NMR spectroscopy measurements also established the presence of interactions in the solution phase.

In general, the strength and high directionality of XB have proven to be successful in reliably organizing the complementary units. As far as the chalcogen bonds are concerned, the current rational design of supramolecular systems is mainly achieved using selenium and tellurium as electrophilic species for strong intermolecular interactions.[73] However, some limitations exist, such as a relatively high sensitivity toward light, oxygen, and certain experimental difficulties associated with (organo)selenium or tellurium chemistry.[74,75] Here, a simple thiophene moiety functionalized at position 3 with pyridyl ring allowed the intermolecular ChB via N···S contacts. Considering the large panel of pyridyl- and thiophenyl-based compounds applied in materials and biological sciences, the rationalization of this intermolecular interaction deserves an ample investigation to obtain critical structural information. Moreover, the halogen and chalcogen bonds can team up and exert a different level of control over the supramolecular organization. Further experiments are however needed to establish a hierarchy among selected XB and ChB donors. More prospectively, the strategy of relying on the combination of both interactions is an appealing approach in designing conducting polymeric materials with complementary donor/acceptor partners and targeting their self-assembly into supramolecular architectures at the nanometer scale.

ASSOCIATED CONTENT

Supporting Information

The Supporting Information is available free of charge at https://pubs.acs.org/doi/10.1021/acs.cgd.2c01402.

Crystallographic data; X-ray structures of complexes of **ThioI**, **ThioPy**−**diIC4**, **ThioI**−**ThioPy A**, and **ThioI**−**ThioPy B**; X-ray powder diffractograms; DSC thermograms; ^{1}H, $^{19}F\{^{1}H\}$, and $^{13}C\{^{1}H\}$ NMR analyses of halogen-bonded complexes; and theoretical methods (PDF)

Accession Codes

CCDC 2172488−2172489 and 2174916−2174923 contain the supplementary crystallographic data for this paper. These data can be obtained free of charge via www.ccdc.cam.ac.uk/data_request/cif, or by emailing data_request@ccdc.cam.ac.uk, or by contacting The Cambridge Crystallographic Data Centre, 12 Union Road, Cambridge CB2 1EZ, UK; fax: +44 1223 336033.

AUTHOR INFORMATION

Corresponding Author

Franck Meyer − *Microbiology, Bioorganic and Macromolecular Chemistry Unit, Faculty of Pharmacy,*

https://doi.org/10.1021/acs.cgd.2c01402
Cryst. Growth Des. XXXX, XXX, XXX−XXX

Université Libre de Bruxelles, 1050 Brussels, Belgium; orcid.org/0000-0002-8028-0609; Email: franck.meyer@ulb.be

Authors

Shiv Kumar − *Microbiology, Bioorganic and Macromolecular Chemistry Unit, Faculty of Pharmacy, Université Libre de Bruxelles, 1050 Brussels, Belgium*

Carole Body − *Institute of Condensed Matter and Nanosciences (IMCN), Université Catholique de Louvain, 1348 Louvain-la-Neuve, Belgium*

Tom Leyssens − *Institute of Condensed Matter and Nanosciences (IMCN), Université Catholique de Louvain, 1348 Louvain-la-Neuve, Belgium;* orcid.org/0000-0001-7916-1373

Kristof Van Hecke − *XStruct, Department of Chemistry, Ghent University, 9000 Ghent, Belgium;* orcid.org/0000-0002-2455-8856

Gilles Berger − *Microbiology, Bioorganic and Macromolecular Chemistry Unit, Faculty of Pharmacy, Université Libre de Bruxelles, 1050 Brussels, Belgium;* orcid.org/0000-0002-5418-9107

Arie Van der Lee − *IEM, Université de Montpellier, CNRS, ENSCM, 34293 Montpellier, France;* orcid.org/0000-0002-4567-1831

Danielle Laurencin − *ICGM, Université de Montpellier, CNRS, ENSCM, 34293 Montpellier, France;* orcid.org/0000-0002-7445-0528

Sébastien Richeter − *ICGM, Université de Montpellier, CNRS, ENSCM, 34293 Montpellier, France;* orcid.org/0000-0001-5284-0931

Sébastien Clément − *ICGM, Université de Montpellier, CNRS, ENSCM, 34293 Montpellier, France;* orcid.org/0000-0002-8473-8197

Complete contact information is available at: https://pubs.acs.org/10.1021/acs.cgd.2c01402

Author Contributions

Conceptualization, F.M.; methodology, F.M. and S.K.; validation, F.M., S.K., C.B., T.L., K.V.H., G.B., A.V.d.L., D.L., S.R., and S.C.; formal analysis, F.M., S.K., C.B., T.L., K.V.H., G.B. A.V.d.L., D.L., S.R., and S.C.; investigation, F.M., S.K., C.B., T.L., K.V.H., G.B. A.V.d.L., D.L., S.R., and S.C.; resources, F.M., T.L., K.V.H., G.B., A.V.d.L., and D.L.; data curation, S.K., C.B., K.V.H., G.B., A.V.d.L., and D.L.; writing—original draft preparation, F.M., S.K., C.B., T.L., K.V.H., G.B., A.V.d.L., D.L., S.R., and S.C.; writing—review and editing, F.M. and S.K.; supervision, F.M.; project administration, F.M.; funding acquisition, F.M.

Funding

F.M. and S.K. thank ULB (PDR 35275398) and FNRS (PDR T.0150.22.F) for the financial support.

Notes

The authors declare no competing financial interest.

■ ACKNOWLEDGMENTS

A.V.d.L., S.R., and S.C. are grateful to the University of Montpellier, the CNRS, and the French Ministry of Research for financial support. S.K. and F.M. thank CIREM for providing NMR infrastructures.

■ REFERENCES

(1) Zhang, D.; Kalaswad, M.; Wang, H. Self-Assembled Vertically Aligned Nanocomposite Systems Integrated on Silicon Substrate: Progress and Future Perspectives. *J. Vac. Sci. Technol., A* **2022**, *40*, 010802.

(2) Han, B.; Li, Z.; Li, C.; Pobelov, I.; Su, G.; Aguilar-Sanchez, R.; Wandlowski, T. From Self-Assembly to Charge Transport with Single From Self-Assembly to Charge Transport with Single Molecules − An Electrochemical Approach. *Top. Curr. Chem.* **2009**, *287*, 181−255.

(3) Chen, Y.; Shu, Z.; Zhang, S.; Zeng, P.; Liang, H.; Zheng, M.; Duan, H. Sub-10 Nm Fabrication: Methods and Applications. *Int. J. Extreme Manuf.* **2021**, *3*, 032002.

(4) Morris, M. A. Directed Self-Assembly of Block Copolymers for Nanocircuitry Fabrication. *Microelectron. Eng.* **2015**, *132*, 207−217.

(5) Cummins, C.; Lundy, R.; Walsh, J. J.; Ponsinet, V.; Fleury, G.; Morris, M. A. Enabling Future Nanomanufacturing through Block Copolymer Self-Assembly: A Review. *Nano Today* **2020**, *35*, 100936.

(6) Lu, W.; Lieber, C. M. Nanoelectronics from the Bottom Up. *Nat. Mater.* **2007**, *6*, 841−850.

(7) Hashemi, D.; Ma, X.; Ansari, R.; Kim, J.; Kieffer, J. Design Principles for the Energy Level Tuning in Donor/Acceptor Conjugated Polymers. *Phys. Chem. Chem. Phys.* **2019**, *21*, 789−799.

(8) Meyer, F. Fluorinated Conjugated Polymers in Organic Bulk Heterojunction Photovoltaic Solar Cells. *Prog. Polym. Sci.* **2015**, *47*, 70−91.

(9) Cavallo, G.; Metrangolo, P.; Milani, R.; Pilati, T.; Priimagi, A.; Resnati, G.; Terraneo, G. The Halogen Bond. *Chem. Rev.* **2016**, *116*, 2478−2601.

(10) Gilday, L. C.; Robinson, S. W.; Barendt, T. A.; Langton, M. J.; Mullaney, B. R.; Beer, P. D. Halogen Bonding in Supramolecular Chemistry. *Chem. Rev.* **2015**, *115*, 7118−7195.

(11) Berger, G.; Soubhye, J.; Meyer, F. Halogen Bonding in Polymer Science: From Crystal Engineering to Functional Supramolecular Polymers and Materials. *Polym. Chem.* **2015**, *6*, 3559−3580.

(12) Berger, G.; Frangville, P.; Meyer, F. Halogen bonding for molecular recognition: new developments in materials and biological sciences. *Chem. Commun.* **2020**, *56*, 4970−4981.

(13) Fourmigué, M.; Batail, P. Activation of Hydrogen- and Halogen-Bonding Interactions in Tetrathiafulvalene-Based Crystalline Molecular Conductors. *Chem. Rev.* **2004**, *104*, 5379−5418.

(14) Bocheux, A.; Tahar-Djebbar, I.; Fiorini-Debuisschert, C.; Douillard, L.; Mathevet, F.; Attias, A.-J.; Charra, F. Self-Templating Polythiophene Derivatives: Electronic Decoupling of Conjugated Strands through Staggered Packing. *Langmuir* **2011**, *27*, 10251−10255.

(15) Abate, A.; Saliba, M.; Hollman, D. J.; Stranks, S. D.; Wojciechowski, K.; Avolio, R.; Grancini, G.; Petrozza, A.; Snaith, H. J. Supramolecular Halogen Bond Passivation of Organic-Inorganic Halide Perovskite Solar Cells. *Nano Lett.* **2014**, *14*, 3247−3254.

(16) Simon, S. J. C.; Parlane, F. G. L.; Swords, W. B.; Kellett, C. W.; Du, C.; Lam, B.; Dean, R. K.; Hu, K.; Meyer, G. J.; Berlinguette, C. P. Halogen Bonding Promotes Higher Dye-Sensitized Solar Cell Photovoltages. *J. Am. Chem. Soc.* **2016**, *138*, 10406−10409.

(17) Barbarella, G.; Melucci, M.; Sotgiu, G. The Versatile Thiophene: An Overview of Recent Research on Thiophene-Based Materials. *Adv. Mater.* **2005**, *17*, 1581−1593.

(18) Zhang, L.; Colella, N. S.; Cherniawski, B. P.; Mannsfeld, S. C. B.; Briseno, A. L. Oligothiophene Semiconductors: Synthesis, Characterization, and Applications for Organic Devices. *ACS Appl. Mater. Interfaces* **2014**, *6*, 5327−5343.

(19) Clément, S.; Meyer, F.; De Winter, J.; Coulembier, O.; Vande Velde, C. M. L.; Zeller, M.; Gerbaux, P.; Balandier, J.-Y.; Sergeyev, S.; Lazzaroni, R.; et al. Synthesis and Supramolecular Organization of Regioregular Polythiophene Block Oligomers. *J. Org. Chem.* **2010**, *75*, 1561.

(20) Zacca, M. J.; Laurencin, D.; Richeter, S.; Clément, S.; Mehdi, A. New Layered Polythiophene-Silica Composite through the Self-Assembly and Polymerization of Thiophene-Based Silylated Molecular Precursors. *Molecules* **2018**, *23*, 2510.

(21) Berger, G.; Soubhye, J.; van der Lee, A.; Vande Velde, C.; Wintjens, R.; Dubois, P.; Clément, S.; Meyer, F. Interplay between Halogen Bonding and Lone Pair-π Interactions: A Computational and Crystal Packing Study. *Chempluschem* **2014**, *79*, 552−558.
(22) Barrès, A.-L.; Allain, M.; Frère, P.; Batail, P. On Dimensionality of Halogen-Bonded Thiophene Solid-State Assemblies. *Isr. J. Chem.* **2014**, *54*, 689−698.
(23) Baldrighi, M.; Metrangolo, P.; Meyer, F.; Pilati, T.; Proserpio, D.; Resnati, G.; Terraneo, G. Halogen-Bonded and Interpenetrated Networks through the Self-Assembly of Diiodoperfluoroarene and Tetrapyridyl Tectons. *J. Fluorine Chem.* **2010**, *131*, 1218−1224.
(24) Widdifield, C. M.; Cavallo, G.; Facey, G. A.; Pilati, T.; Lin, J.; Metrangolo, P.; Resnati, G.; Bryce, D. L. Multinuclear Solid-State Magnetic Resonance as a Sensitive Probe of Structural Changes upon the Occurrence of Halogen Bonding in Co-Crystals. *Chem.—Eur. J.* **2013**, *19*, 11949−11962.
(25) Bryce, D. L.; Viger-Gravel, J. Solid-State NMR Study of Halogen-Bonded Adducts. *Top. Curr. Chem.* **2008**, *358*, 183−203.
(26) *Rigaku Oxford Diffraction, CrysAlisPro Software Systems*; Rigaku Corporation: Oxford, U.K., 2012.
(27) van der Lee, A. Charge Flipping for Routine Structure Solution. *J. Appl. Crystallogr.* **2013**, *46*, 1306−1315.
(28) Palatinus, L.; Chapuis, G. SUPERFLIP- a computer program for the solution of crystal structures by charge flipping in arbitrary dimensions. *J. Appl. Crystallogr.* **2007**, *40*, 786−790.
(29) Betteridge, P. W.; Carruthers, J. R.; Cooper, R. I.; Prout, K.; Watkin, D. J. CRYSTALSversion 12: software for guided crystal structure analysis. *J. Appl. Crystallogr.* **2003**, *36*, 1487.
(30) *Rigaku Oxford Diffraction, CrysAlisPro Software Systems*; Rigaku Corporation, Oxford, U.K.: 2019.
(31) Dolomanov, O. V.; Bourhis, L. J.; Gildea, R. J.; Howard, J. A. K.; Puschmann, H. OLEX2: A Complete Structure Solution, Refinement and Analysis Program. *J. Appl. Crystallogr.* **2009**, *42*, 339−341.
(32) Sheldrick, G. M. SHELXT- Integrated space-group and crystal-structure determination. *Acta Crystallogr., Sect. A: Found. Crystallogr.* **2015**, *71*, 3−8.
(33) Sheldrick, G. M. Crystal structure refinement withSHELXL. *Acta Crystallogr., Sect. C: Struct. Chem.* **2015**, *71*, 3−8.
(34) Neese, F. The ORCA Program System. *Wiley Interdiscip. Rev.: Comput. Mol. Sci.* **2012**, *2*, 73−78.
(35) Neese, F. Software Update: The ORCA Program System—Version 5.0. *Wiley Interdiscip. Rev.: Comput. Mol. Sci.* **2022**, *12*, No. e1606.
(36) Riplinger, C.; Neese, F. An Efficient and near Linear Scaling Pair Natural Orbital Based Local Coupled Cluster Method. *J. Chem. Phys.* **2013**, *138*, 034106.
(37) Schneider, W. B.; Bistoni, G.; Sparta, M.; Saitow, M.; Riplinger, C.; Auer, A. A.; Neese, F. Decomposition of Intermolecular Interaction Energies within the Local Pair Natural Orbital Coupled Cluster Framework. *J. Chem. Theory Comput.* **2016**, *12*, 4778−4792.
(38) Weigend, F. Accurate Coulomb-Fitting Basis Sets for H to Rn. *Phys. Chem. Chem. Phys.* **2006**, *8*, 1057−1065.
(39) Arman, H. D.; Gieseking, R. L.; Hanks, T. W.; Pennington, W. T. Complementary halogen and hydrogen bonding: sulfur···iodine interactions and thioamide ribbons. *Chem. Commun.* **2010**, *46*, 1854−1856.
(40) Haberhauer, G.; Gleiter, R. The Nature of Strong Chalcogen Bonds Involving Chalcogen-Containing Heterocycles. *Angew. Chem., Int. Ed.* **2020**, *59*, 21236−21243.
(41) Kumar, V.; Pilati, T.; Terraneo, G.; Meyer, F.; Metrangolo, P.; Resnati, G. Halogen bonded Borromean networks by design: topology invariance and metric tuning in a library of multi-component systems. *Chem. Sci.* **2017**, *8*, 1801−1810.
(42) Ding, X.; Chang, Y.; Ou, C.; Lin, J.; Xie, L.; Huang, W. Halogen bonding in the co-crystallization of potentially ditopic diiodotetra-fluorobenzene: a powerful tool for constructing multicomponent supramolecular assemblies. *Natl. Sci. Rev.* **2020**, *7*, 1906−1932.
(43) Chu, M.; Qiu, B.; Zhang, W.; Zhou, Z.; Yang, X.; Yan, Y.; Yao, J.; Li, Y. J.; Zhao, Y. S. Tailoring the Energy Levels and Cavity Structures toward Organic Cocrystal Microlasers. *ACS Appl. Mater. Interfaces* **2018**, *10*, 42740−42746.
(44) Bai, L.; Bose, P.; Gao, Q.; Li, Y.; Ganguly, R.; Zhao, Y. Halogen-Assisted Piezochromic Supramolecular Assemblies for Versatile Haptic Memory. *J. Am. Chem. Soc.* **2017**, *139*, 436−441.
(45) Berger, G.; Robeyns, K.; Soubhye, J.; Wintjens, R.; Meyer, F. Halogen Bonding in a Multi-Connected 1,2,2-Triiodo-Alkene Involving Geminal and/or Vicinal Iodines: A Crystallographic and DFT Study. *CrystEngComm* **2016**, *18*, 683−690.
(46) Gao, Y. J.; Li, C.; Liu, R.; Jin, W. J. Phosphorescence of several cocrystals assembled by diiodotetrafluorobenzene and three ring angular diazaphenanthrenes via C I··· N halogen bond. *Spectrochim. Acta, Part A* **2017**, *173*, 792−799.
(47) Chen, Y.; Huang, S.; Wang, T.; Yu, H. Enhanced Ordering and Efficient Photoalignment of Nanostructures in Block Copolymers Enabled by Halogen Bond. *Macromolecules* **2020**, *53*, 1486−1493.
(48) Du, M.; Li, L.; Zhang, J.; Li, K.; Cao, M.; Mo, L.; Hu, G.; Chen, Y.; Yu, H.; Yang, H. Photoresponsive iodine-bonded liquid crystals based on azopyridine derivatives with a low phase-transition temperature. *Liq. Cryst.* **2019**, *46*, 37−44.
(49) Shen, Q. J.; Wei, H. Q.; Zou, W. S.; Sun, H. L.; Jin, W. J. Cocrystals Assembled by Pyrene and 1,2- or 1,4-Diiodotetrafluor-obenzenes and Their Phosphorescent Behaviors Modulated by Local Molecular Environment. *CrystEngComm* **2012**, *14*, 1010−1015.
(50) Metrangolo, P.; Murray, J. S.; Pilati, T.; Politzer, P.; Resnati, G.; Terraneo, G. Fluorine-Centered Halogen Bonding: A Factor in Recognition Phenomena and Reactivity. *Cryst. Growth Des.* **2011**, *11*, 4238−4246.
(51) Pavan, M. S.; Durga Prasad, K. D.; Guru Row, T. N. G. Halogen bonding in fluorine: experimental charge density study on intermolecular F···F and F···S donor-acceptor contacts. *Chem. Commun.* **2013**, *49*, 7558−7560.
(52) Eskandari, K.; Lesani, M. Does Fluorine Participate in Halogen Bonding? *Chem.—Eur. J.* **2015**, *21*, 4739−4746.
(53) Fonseca, T. A. O.; Freitas, M. P.; Cormanich, R. A.; Ramalho, T. C.; Tormena, C. F.; Rittner, R. Computational evidence for intramolecular hydrogen bonding and nonbonding X···O interactions in 2'-haloflavonols. *Beilstein J. Org. Chem.* **2012**, *8*, 112−117.
(54) Elakkat, V.; Chang, C.-C.; Chen, J.-Y.; Fang, Y.-C.; Shen, C.-R.; Liu, L.-K.; Lu, N. The First Two Examples of Halogen Bonding with a Sigma Hole-Donating Fluorine in the Csp3−F Osp3 Interaction from Polyfluorinated Trans-Dihalopalladium(II) Di-Substituted Pyridine Complexes. *Chem. Commun.* **2019**, *55*, 14259−14262.
(55) Spackman, M. A.; Jayatilaka, D. Hirshfeld Surface Analysis. *CrystEngComm* **2009**, *11*, 19−32.
(56) Scilabra, P.; Terraneo, G.; Resnati, G. The Chalcogen Bond in Crystalline Solids: A World Parallel to Halogen Bond. *Acc. Chem. Res.* **2019**, *52*, 1313−1324.
(57) Koebel, M. R.; Cooper, A.; Schmadeke, G.; Jeon, S.; Narayan, M.; Sirimulla, S. S···O and S···N Sulfur Bonding Interactions in Protein-Ligand Complexes: Empirical Considerations and Scoring Function. *J. Chem. Inf. Model.* **2016**, *56*, 2298−2309.
(58) Lim, J. Y. C.; Beer, P. D. Sigma-Hole Interactions in Anion Recognition. *Chem* **2018**, *4*, 731−783.
(59) Réthoré, C.; Madalan, A.; Fourmigué, M.; Canadell, E.; Elsa, B.; Almeida, M.; Clérac, R.; Avarvari, N. OS vs . NS Intramolecular Nonbonded Interactions in Neutral and Radical Cation Salts of TTF-Oxazoline Derivatives : Synthesis , Theoretical Investigations , Crystalline Structures , and Physical Properties. *New J. Chem.* **2007**, *31*, 1468−1483.
(60) Suresh, K.; Minkov, V. S.; Namila, K. K.; Derevyannikova, E.; Losev, E.; Nangia, A.; Boldyreva, V. Novel Synthons in Sulfamethizole Cocrystals: Structure-Property Relations and Solubility. *Cryst. Growth Des.* **2015**, *15*, 3498−3510.
(61) Mondal, P. K.; Rao, V.; Mittapalli, S.; Chopra, D. Exploring Solid State Diversity and Solution Characteristics in a Fluorine-Containing Drug Riluzole. *Cryst. Growth Des.* **2017**, *17*, 1938−1946.

https://doi.org/10.1021/acs.cgd.2c01402
Cryst. Growth Des. XXXX, XXX, XXX−XXX

(62) Sesto, R. E. D.; Botoshansky, M.; Kaftory, M.; Arif, A. M.; Miller, J. S. Charge Transfer Complexes of 2,4,6-Tricyano-s-Triazine with Tetrathiafulvalene (TTF) and Y,\,Y,V-Tetramethyl-/j-Phenyl-enediamine (TMPD). *CrystEngComm* **2002**, *4*, 117−120.
(63) Sarmah, K. K.; Nath, N.; Rao, D. R.; Thakuria, R. Mechanochemical Synthesis of Drug-Drug and Drug-Nutraceutical Multicomponent Solids of Olanzapine. *CrystEngComm* **2020**, *22*, 1120−1130.
(64) Sakai, K.; Nagahara, K.; Yoshii, Y.; Hoshino, N.; Akutagawa, T. Structural and Spectroscopic Study of 6,7-Dicyano-Substituted Lumazine with High Electron Affinity and Proton Acidity. *J. Phys. Chem. A* **2013**, *117*, 3614−3624.
(65) Avvakumov, E.; Senna, M.; Kosova, N. *Soft Mechanochemical Synthesis: A Basis for New Chemical Technologies*; Kluwer Academic Publishers, 2001.
(66) Mayer, U.; Gutmann, V.; Gerger, W. The acceptor number ? A quantitative empirical parameter for the electrophilic properties of solvents. *Monatsh. Chem.* **1975**, *106*, 1235−1257.
(67) Hyun, B. R.; Bartnik, A. C.; Lee, J. K.; Imoto, H.; Sun, L.; Choi, J. J.; Chujo, Y.; Hanrath, T.; Ober, C. K.; Wise, F. W. Role of Solvent Dielectric Properties on Charge Transfer from PbS Nanocrystals to Molecules. *Nano Lett.* **2010**, *10*, 318−323.
(68) Xu, Y.; Szell, P. M. J.; Kumar, V.; Bryce, D. L. Solid-State NMR Spectroscopy for the Analysis of Element-Based Non-Covalent Interactions. *Coord. Chem. Rev.* **2020**, *411*, 213237.
(69) Vioglio, P. C.; Chierotti, M. R.; Gobetto, R. Solid-state nuclear magnetic resonance as a tool for investigating the halogen bond. *CrystEngComm* **2016**, *18*, 9173−9184.
(70) Viger-Gravel, J.; Leclerc, S.; Korobkov, I.; Bryce, D. L. Correlation between 13C Chemical Shifts and the Halogen Bonding Environment in a Series of Solid Para-Diiodotetrafluorobenzene Complexes. *CrystEngComm* **2013**, *15*, 3168−3177.
(71) Frangville, P.; Kumar, S.; Gelbcke, M.; Van Hecke, K.; Meyer, F. Stimuli Responsive Materials Supported by Orthogonal Hydrogen and Halogen Bonding or I ··· Alkene Interaction. *Molecules* **2021**, *26*, 07586.
(72) Ma, N.; Zhang, Y.; Ji, B.; Tian, A.; Wang, W. Structural Competition between Halogen Bonds and Lone-Pair···π Interactions in Solution. *ChemPhysChem* **2012**, *13*, 1411−1414.
(73) Vogel, L.; Wonner, P.; Huber, S. M. Chalcogen Bonding: An Overview. *Angew. Chem., Int. Ed.* **2019**, *58*, 1880−1891.
(74) Mukherjee, A. J.; Zade, S. S.; Singh, H. B.; Sunoj, R. B. Organoselenium Chemistry: Role of Intramolecular Interactions. *Chem. Rev.* **2010**, *110*, 4357−4416.
(75) Chivers, T.; Laitinen, R. S. Tellurium: A Maverick among the Chalcogens. *Chem. Soc. Rev.* **2015**, *44*, 1725−1739.

https://doi.org/10.1021/acs.cgd.2c01402
Cryst. Growth Des. XXXX, XXX, XXX−XXX